



# Critical exponents of a self-propelled particles system

Dorilson S. Cambui<sup>a,b,\*</sup>, Alberto S. de Arruda<sup>c</sup>, Maurício Godoy<sup>c</sup>

<sup>a</sup> Secretaria de Estado de Educação de Mato Grosso, 78049-909, Cuiabá, Mato Grosso, Brazil

<sup>b</sup> Universidade do Estado de Mato Grosso, UNEMAT, Departamento de Matemática, Barra do Bugres, Mato Grosso, Brazil

<sup>c</sup> Instituto de Física, Universidade Federal de Mato Grosso, 78060-900, Cuiabá, MT, Brazil

## HIGHLIGHTS

- We model self-propelled particles system used to study the live organisms motion.
- Important parameters in this system are velocity, interaction radius and density.
- We estimate a set of critical exponents as a function of these parameters.
- We find that such parameters, in turn, influences the values of critical exponents.
- Critical exponents obtained satisfy the hyperscaling relationship.

## ARTICLE INFO

### Article history:

Received 4 May 2015

Received in revised form 22 September

2015

Available online 24 October 2015

### Keywords:

Self-propelled particles

Collective motion

Finite-size scaling

Phase transition

Critical exponents

## ABSTRACT

The Vicsek model of self-propelled particles is an important tool in the study of the collective motion of live organisms. The model consists of particles that move with a constant velocity and adopt, in a region called the zone of repulsion, the average motion direction of their neighbors disturbed by an external noise. A second-order phase transition from a disordered state, with motion in random directions, to an ordered motion state was observed. In this work, we have estimated, using finite-size scaling arguments, the critical exponents  $\beta$ ,  $\gamma$  and  $\nu$  of the original Vicsek model as a function of parameters important to the model, such as the orientation radius size, density, and velocity modulus. Our results show that the critical exponents depend greatly on these parameters.

© 2015 Elsevier B.V. All rights reserved.

## 1. Introduction

Collective behavior is a fascinating characteristic observed in biological systems [1]. Examples of organized animal groups observed in nature include flocks of birds [2], herds of mammals [3], and schools of fish [4]. In these aggregates, global collective behavior emerges as a result of the local interactions among individuals in close proximity to one another where each individual in the group engages in behavior as a function of the position and velocity of its nearest neighbors and, as a natural consequence, aligns itself and moves in a common direction. In this context, several studies have been employed in order to describe the main features of collective motion in such systems [5–12]. Self-propelled particle dynamics was employed by Vicsek et al. [5] to describe the collective phenomena of biological organisms. In their model, each particle moves with a constant velocity and at each time step adopts the average motion direction of its neighboring within an interaction radius  $r$  centered at the actual position of the particle. The particles that access this interaction zone will have their directions updated with some random perturbation added to their motion. When noise is introduced, the Vicsek model

\* Corresponding author at: Secretaria de Estado de Educação de Mato Grosso, 78049-909, Cuiabá, Mato Grosso, Brazil.

E-mail address: [dcambui@fisica.ufmt.br](mailto:dcambui@fisica.ufmt.br) (D.S. Cambui).

displays a phase transition, controlled by the noise intensity, a phase transition from a disordered state, with random motion directions, to an ordered state wherein the individuals move coherently in the same common direction. In their work, Vicsek et al. classify the nature of this transition as second-order, which was later confirmed by other authors [13,14].

Random perturbations in the motion direction in self-propelled models represent errors committed by the particles in evaluating the real motion direction of its neighbors. There are two types of noise—intrinsic and extrinsic, also referred to as angular and vectorial respectively. We can define intrinsic noise as arising from the errors committed when particles try to follow the average motion direction, already perfectly calculated, of neighboring particles. On the other hand, for the case of extrinsic or vectorial noise the errors arise from the evaluation of each particle–particle interaction; in this case, the noise is added directly into the interactions between the particle  $i$  and each one of its neighbors. The two different ways in which the noise is introduced produces different types of phase transitions. The orientational transition in the Vicsek model with intrinsic noise was shown to have a continuous character, whereas models with extrinsic noise have been shown to lead to a discontinuous phase transition.

Although the study of self-propelled particles systems is well established in the literature, we are not aware of a detailed study of critical exponents. Vicsek et al. [5] calculated the critical exponent associated with the order parameter and found  $\beta = 0.45(7)$ , for a given density  $\rho = 0.4$  and a velocity  $v_0 = 0.03$ . They did not consider the exponents  $\nu$  and  $\gamma$ , of correlation length and susceptibility respectively. In a more thorough analysis using finite-size scaling arguments, Baglietto and Albano [15] obtained, by collapsing data onto a single curve, the static exponents of Vicsek model for systems of different sizes and densities in the low-velocity regime. They found  $\beta = 0.45(3)$ ,  $\gamma = 2.3(4)$  and  $\nu = 1.6(3)$ . Important results were found in Refs. [14,16], where the coupled effect between initial velocity and density of particles has been shown to play an important role in changing the behavior of order parameter. In this same context, Tarras et al. [17] proposed a Vicsek-type model, where they added a repulsion zone in order to avoid collisions between the particles. They calculated the critical exponents  $\beta$  and  $\delta$  for different repulsion radiuses and densities and showed that exponents depend greatly on the size of these parameters, indeed the model proposed by them indicate the non-universality of these exponents.

Important parameters in the original Vicsek model are: the velocity of particles, the interaction radius, and the density. High velocities can speed up the interactions; the gradual increase of the interaction radius increases the number of neighbors of each particle contributing to group cohesion; and large densities contribute to the appearance of ordered motion.

Our contribution in this paper is to estimate the static critical exponents of the original Vicsek model as a function of density, velocity and orientation radius. We employ finite-size scaling arguments in order to obtain a complete picture in terms of each of these parameters. We have demonstrated that the values of parameters  $\rho$ ,  $r$  and  $v_0$  influence significantly the values of the critical exponents, indicating that the critical exponents depend on the details of the model.

The rest of this paper is organized as follows: The detailed formulation of the Vicsek model [5] is presented in Section 2. In Section 3, the simulation parameters and a brief description of the finite-size scaling theory is discussed. We present the results of our simulations in Section 4 and the main conclusions are presented in Section 5.

## 2. The Vicsek model—a brief description

In a two-dimensional space, initially  $N$  self-propelled particles are characterized by their position vector  $\mathbf{x}_i(t)$  in  $t$  time. Their directions are distributed randomly in a square lattice  $L$ , with periodic boundary conditions and a constant velocity ( $v_0 = 0.03$ ). The interactions between particles occur, at each time step, in a region of radius  $r = 1$ , where each individual particle assumes the average motion direction of all its neighbors. The positions are updated by the equation,

$$\mathbf{x}_i(t + \tau) = \mathbf{x}_i(t) + \mathbf{v}_i(t)\tau, \quad (1)$$

where  $\tau = 1$  is the time interval. The direction of an individual particle  $i$ , with some uncertainty, is specified by the angle  $\theta_i(t + \tau)$ , which is updated by the following interaction rule,

$$\theta_i(t + \tau) = \langle \theta(t) \rangle_{(r=1)} + \xi(t) \times \eta \quad (2)$$

where  $\langle \theta(t) \rangle_{(r=1)}$  denotes the average motion direction of the neighboring particles,  $\xi$  is a random variable uniformly distributed between  $[-\pi, \pi]$ , and  $\eta$  is the strength of noise.

The order parameter  $\psi$  is defined as the absolute value of the normalized average velocity, i.e.,

$$\psi = \frac{1}{Nv_0} \left| \sum_{i=1}^N \mathbf{v}_i(t) \right|, \quad (3)$$

where  $\psi$  varies between  $[0, 1]$ .  $\psi$  is zero when the motion directions of the particles are random, in this case no average alignment of the velocities is verified. When  $\psi$  equals one, the particles tend to move towards the same direction. The shape of the curve of  $\psi$  (see Fig. 1) suggests, as pointed out in Ref. [5], the presence of a second-order phase transition in the system.

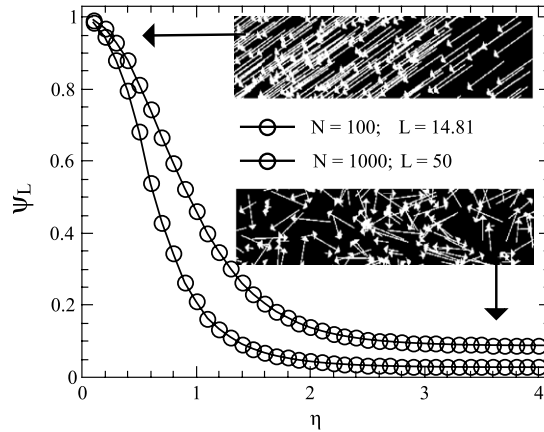


**Fig. 1.** Order parameter  $\psi_L$  versus the noise  $\eta$ , in two different system sizes as indicated in the figure and with fixed density  $\rho = 0.4$ .

### 3. Simulations parameters and finite-size scaling analysis

We performed a series of numerical simulations changing the density  $\rho$ , the velocity  $v_0$ , and the interaction radius  $r$  (where directional alignment occurs between particles), in order to obtain the critical exponents of the system as a function of each of these parameters. Our simulation starts with a random configuration of the positions and directions of each particle. We have adopted periodic boundary conditions, discrete time step  $\tau = 1$ , and fixed values of the number of particles  $N = 100, 200, 300, 500$  and  $1000$ .

To find the critical exponents as a function of the density, we have considered the following values:  $\rho = 0.1, 0.2, 0.4, 1, 2, 4, 6, 8$  and  $10$ . For each  $\rho$  the lattice size is  $L = \sqrt{(N/\rho)}$ , with  $r = 1$  and  $v_0 = 0.03$ . We are also interested in estimating the critical exponents as a function of the magnitude of velocity. To this end, we considered values between a low velocity configuration (with  $v_0 = 0.03, 0.1$  and  $0.5$ ) and a high velocity configuration ( $v_0 = 5$  and  $10$ ). In both cases, we maintained the fixed density for  $\rho = 0.4$  with  $r = 1$ . Finally, in order to obtain the critical exponents in terms of interaction radius  $r$ , we assume  $r = 1, 2, 4, 6, 8$  and  $10$ , for the same fixed density  $\rho = 0.4$  with  $v_0 = 0.03$ . All of our data were obtained over  $1.5 \times 10^6$  time steps to estimate the average values of the quantities of interest with a relaxation time of  $1 \times 10^4$ .

In equilibrium critical phenomena, finite-size scaling (FSS) is a very useful technique to find the correct values of the critical exponents. The Vicsek model is known to be a non-equilibrium system, but the critical exponents of the model can be obtained via FSS [15]. In this work, we employed finite-size scaling arguments [18,19] to estimate the values of static critical exponents  $\beta$ ,  $\nu$  and  $\gamma$  at the critical point of the system.  $\beta$  is the order parameter critical exponent,  $\nu$  is the correlation-length critical exponent (which measures correlations of the order parameter  $\psi$ , defined by Eq. (3)), and  $\gamma$  is the susceptibility  $\chi$  critical exponent. The susceptibility is characterized by a peak near the critical point and it is defined as [15],

$$\chi = L^2 (\langle \psi^2 \rangle - \langle \psi \rangle^2), \quad (4)$$

where  $(\langle \psi^2 \rangle - \langle \psi \rangle^2)$  is the order parameter variance. To determine the critical exponent  $\nu$ , we used the fourth-order Binder cumulant [18,19],

$$C = 1 - \frac{\langle \psi^4 \rangle}{3 \langle \psi^2 \rangle^2}. \quad (5)$$

In the neighborhood of the stationary critical point  $\eta_c$ , all quantities defined by Eqs. (3)–(5) obey the following finite-size scaling relations [18,19],

$$\psi_L(\eta) = L^{-\beta/\nu} \psi_{\pm}(L^{1/\nu} \varepsilon), \quad (6)$$

$$\chi_L(\eta) = L^{\gamma/\nu} \chi_{\pm}(L^{1/\nu} \varepsilon), \quad (7)$$

$$C_L(\eta) = C_{\pm}(L^{1/\nu} \varepsilon), \quad (8)$$

where  $\eta_c$  is the critical noise,  $\varepsilon = (\eta - \eta_c)/\eta_c$ ,  $\psi_{\pm}$ ,  $\chi_{\pm}$  and  $C_{\pm}$  are scaling functions and  $+$  or  $-$  index refers to  $\eta > \eta_c$  and  $\eta < \eta_c$ , respectively. To estimate the critical exponent  $\nu$ , we perform the derivative of Eq. (8) with respect to the noise  $\eta$  and we obtain the following scaling relation [20],

$$C'_L(\eta) = L^{1/\nu} \frac{C'_{\pm}(L^{1/\nu} \varepsilon)}{\eta_c}. \quad (9)$$

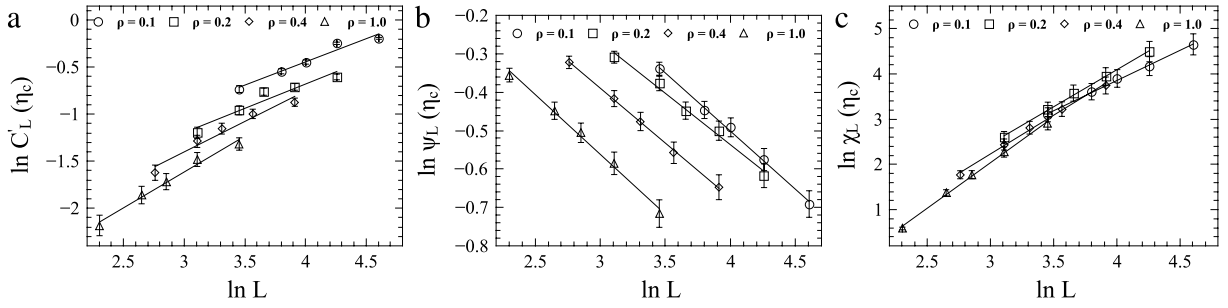


**Fig. 2.** Log-log plots of (a)  $C'_L$ , (b)  $\psi_L$  and (c)  $\chi_L$  as a function of the linear lattice size, at the critical point  $\eta_c$  and for several values of  $\rho$  as indicated in the figure. The straight lines are the best fit to the data points. All data are for  $v_0 = 0.03$  and  $r = 1$ .

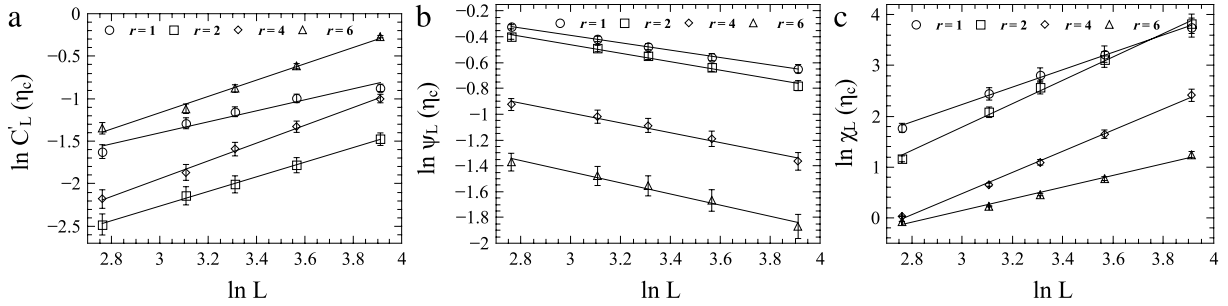


**Fig. 3.** Log-log plots of (a)  $C'_L$ , (b)  $\psi_L$  and (c)  $\chi_L$  as a function of the linear lattice size, at the critical point  $\eta_c$  and for several values of  $r$  as indicated in the figure. The straight lines are the best fit to the data points. All data are for  $v_0 = 0.03$  and  $\rho = 0.4$ .

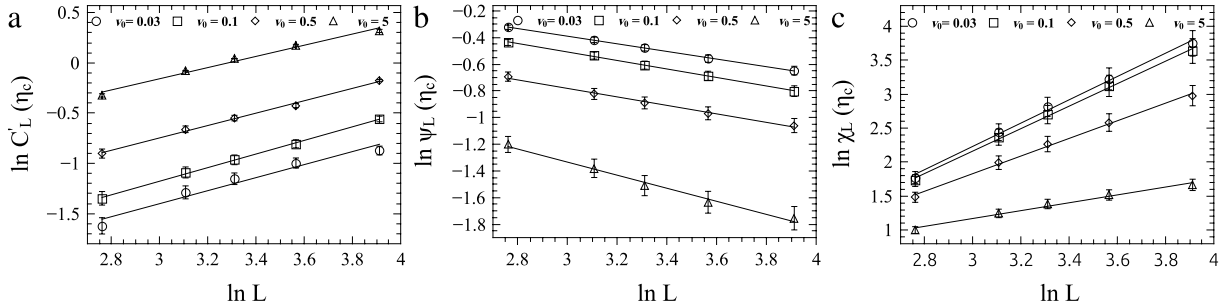


**Fig. 4.** Log-log plots of (a)  $C'_L$ , (b)  $\psi_L$  and (c)  $\chi_L$  as a function of the linear lattice size, at the critical point  $\eta_c$  and for several values of  $v_0$  as indicated in the figure. The straight lines are the best fit to the data points. All data are for  $\rho = 0.4$  and  $r = 1$ .

Finally, at the critical point, the relations (6), (7) and (9) yield,

$$\psi_L(\eta_c) = L^{-\beta/\nu} \psi_{\pm}(0), \quad (10)$$

$$\chi_L(\eta_c) = L^{\gamma/\nu} \chi_{\pm}(0), \quad (11)$$

$$C'_L(\eta_c) = L^{1/\nu} \frac{C'_{\pm}(0)}{\eta_c}. \quad (12)$$

From the log-log plots of  $C'_L(\eta_c)$ ,  $\psi_L(\eta_c)$  and  $\chi_L(\eta_c)$  versus  $L$ , at the critical point, we found the critical ratios  $1/\nu$ ,  $\beta/\nu$ ,  $\gamma/\nu$ . In order to estimate the critical noise, we used the peak position of the susceptibility  $\chi_L$ ; the position of the peaks can be defined at a pseudocritical noise  $\eta_{\max}(L)$ , which approaches  $\eta_c$  when  $L \rightarrow \infty$ .

#### 4. Results

Finite-size effects of the order parameter were studied as a function of some values of the density  $\rho$ , of the size of orientation radius  $r$ , and of the velocity  $v_0$ . Upon variation of these parameters, Figs. 2–4 display log-log plots of  $\psi_L$ ,  $\chi_L$  and  $C'_L$ , given by Eqs. (10)–(12), as a function of the linear size  $L$  at the critical point of the system. The error bar for each point is included in these plots.

**Table 1**

Critical noise and exponents as a function of density  $\rho$  with following parameters:  $r = 1$ ,  $v_0 = 0.03$ .

$\rho$	$\eta_c$	$\nu$	$\beta$	$\beta/\nu$	$\gamma$	$\gamma/\nu$
0.1	0.32	2.03(2)	0.61(9)	0.31(2)	2.7(4)	1.33(4)
0.2	0.42	1.93(2)	0.52(9)	0.27(1)	3.17(4)	1.63(4)
0.4	0.62	1.54(2)	0.44(6)	0.28(5)	2.64(4)	1.71(6)
1	1.04	1.31(9)	0.41(4)	0.31(1)	2.64(2)	2.01(6)
2	1.50	1.04(6)	0.34(4)	0.33(2)	2.44(2)	2.34(8)
4	2.14	0.93(3)	0.31(3)	0.34(2)	2.16(9)	2.33(2)
6	2.55	1.13(1)	0.38(5)	0.34(1)	1.91(4)	1.70(1)
8	2.77	0.94(3)	0.39(4)	0.41(3)	1.62(7)	1.72(2)
10	2.92	0.97(3)	0.41(5)	0.42(3)	1.39(8)	1.43(3)

**Table 2**

Critical noise and exponents as a function of the interaction radius size  $r$  with following parameters:  $\rho = 0.4$  and  $v_0 = 0.03$ .

$\rho$	$\eta_c$	$\nu$	$\beta$	$\beta/\nu$	$\gamma$	$\gamma/\nu$
1	0.62	1.54(2)	0.44(6)	0.28(5)	2.64(4)	1.71(6)
2	1.35	1.16(3)	0.38(3)	0.33(2)	2.67(2)	2.30(1)
4	2.59	0.95(3)	0.36(4)	0.38(3)	1.99(1)	2.08(6)
6	3.11	1.04(5)	0.45(6)	0.43(4)	1.20(1)	1.15(1)
8	3.36	1.27(6)	0.57(6)	0.45(3)	1.17(1)	0.91(8)
10	3.50	1.40(1)	0.65(1)	0.46(3)	0.81(2)	0.57(6)

**Table 3**

Values for the critical noise and exponents as a function of the velocity modulus  $v_0$  with following parameters:  $r = 1$  and  $\rho = 0.4$ .

$\rho$	$\eta_c$	$\nu$	$\beta$	$\beta/\nu$	$\gamma$	$\gamma/\nu$
0.03	0.62	1.54(2)	0.44(6)	0.28(5)	2.64(4)	1.71(6)
0.1	0.74	1.48(3)	0.47(2)	0.32(1)	2.44(1)	1.65(4)
0.5	1.09	1.62(6)	0.52(4)	0.32(3)	2.10(1)	1.29(2)
5	1.59	1.79(4)	0.88(7)	0.49(2)	1.04(9)	0.58(4)
10	1.60	1.80(2)	0.80(9)	0.44(1)	1.02(1)	0.57(1)

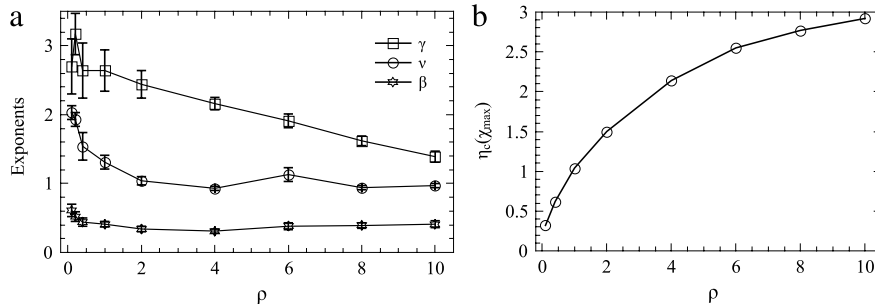


**Fig. 5.** (a) Critical exponents  $\gamma$ ,  $\nu$  and  $\beta$ ; (b) critical noise  $\eta_c$ , as a function of the density.

The results of our simulations show that the critical exponents obtained by the original Vicsek model for self-propelled particles display a dependence as the density, the velocity and the interaction radius. Therefore, we observed that the critical exponents obtained in such a system can lead to a non-universality class. In fact, this result was expected, since Ref. [17] demonstrated this same behavior for the critical exponents (associated to order parameter)  $\beta$  and  $\delta$ . However, the model they considered was not the Vicsek model in its original formulation with only one interaction rule, namely, the directional alignment, but rather a variation of the Vicsek model. They incorporated into their simulations, in addition to the rule of velocity alignment, a second interaction zone, called the repulsion zone, where the direction of motion of a particle is generated by repulsive interactions with other neighboring individual particles.

The results we found for the critical noise as well as for the critical exponents (given by the slope of the curves in Figs. 2–4 are summarized in Tables 1–3). These quantities also were plotted as a function of the parameters  $\rho$ ,  $r$  and  $v_0$ , as can be seen in Figs. 5–7, where the behavior of the curves (Figs. 5(a), 6(a) and 7(a)) indicates that the critical exponents of a self-propelled particles system are non-universality.

To understand why the exponents vary with the parameters  $\rho$ ,  $r$  and  $v_0$ , Fig. 8 shows the effects that these parameters can have on the system. In these figures we exhibit the polarization  $p$ , which gives the arithmetic mean deviation of an angle

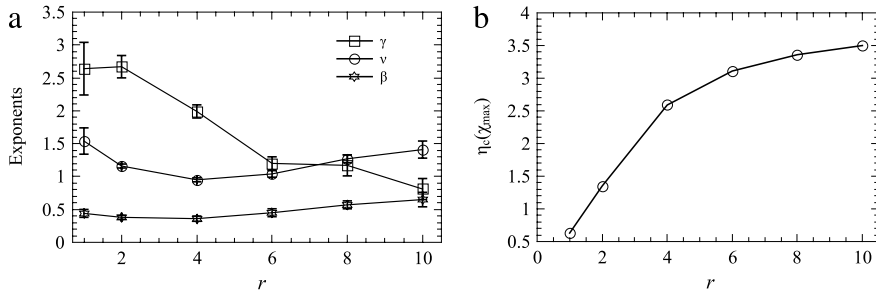


**Fig. 6.** (a) Critical exponents  $\gamma$ ,  $\nu$  and  $\beta$ ; (b) critical noise  $\eta_c$ , as a function of the interaction radius.

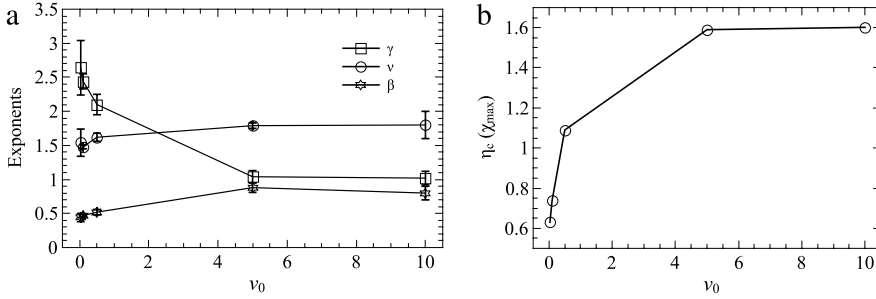


**Fig. 7.** (a) Critical exponents  $\gamma$ ,  $\nu$  and  $\beta$ ; (b) critical noise  $\eta_c$ , as a function of the velocity modulus.

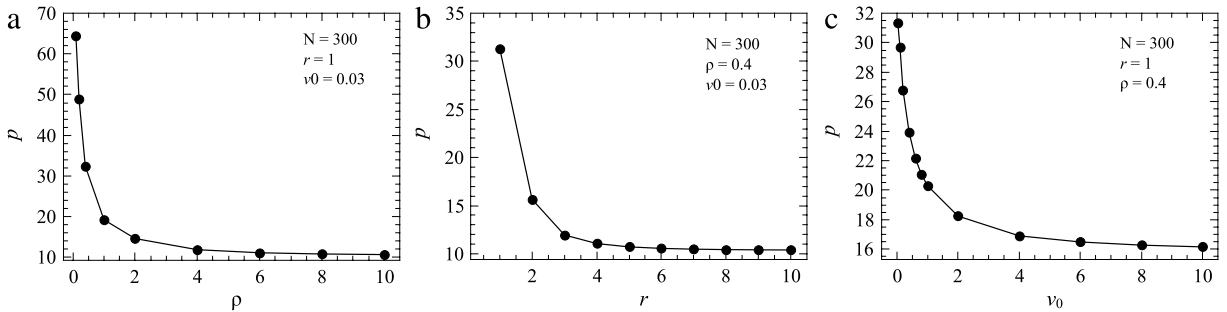


**Fig. 8.** Dependence of the polarization  $p$  versus: (a) the density; (b) the interaction radius, and (c) the velocity modulus.

of a particle in relation to the total group of particles, defined by,

$$p = \left[ \frac{\mathbf{v}_i}{|\mathbf{v}_i|}, \sum_{i=1}^N \frac{\mathbf{v}_i}{|\mathbf{v}_i|} \right], \quad (13)$$

where the first term of Eq. (13) represents the direction of the velocity of each particle  $i$ . In the second term we have the direction of the velocities of the total group of particles. Therefore,  $p$  quantifies the intensity of the orientation and may assume values between  $0^\circ$  and  $90^\circ$ ;  $p = 0^\circ$  indicates that the particles within the group have ordered their motions, and for  $p = 90^\circ$  we have a configuration in which the particles are in a completely unaligned state with respect to their motion directions. We can observe that the variation of these parameters influences collective motion considerably. This is because the parameters affect the intensity of the directional alignment of the particles. For lowest values  $\rho$ ,  $r$  and  $v_0$ , there is greater deviation of the orientation of each agent from the average direction of the group. On the other hand, the directional order is gradually pronounced for the higher values, indicating that, as a function of each of these parameters, the system undergoes a phase transition from a disordered state to an ordered state. In Fig. 8, the ordered state is more pronounced because the interaction between the particles is greater; the increase in density decreases the distance between particles contributing to greater interaction, while high velocities can speed up the interactions. Also, the increase of the interaction radius leads to a larger number of interacting particles. Then the critical exponents depend on the details of the model and the non-universality involves the range of the interactions [21] between particles.

## 5. Conclusions

In this work, we have applied the standard finite-size scaling techniques (FSS) taken from the theory of equilibrium phase transitions. Using our approach we obtained a complete set of static critical exponents of the Vicsek model for self-propelled particles. We analyzed three particular cases where we varied the density  $\rho$  of particles, the interaction radius  $r$ , and the velocity  $v_0$ . Our results indicate that this parameter influences significantly the values of the critical exponents, which tend to vary with respect to the values of  $\rho$ ,  $r$  and  $v_0$ . In order to understand the reason for this tendency, we investigated the effects of these parameters on the directional alignment of self-propelled particles through calculus of the polarization  $p$ , which quantifies (in degrees) the intensity of the directional orientation between the particles. The higher values of  $p$  indicate greater disorder. We found that collective motion is greatly affected by the variation of these parameters (ordered motion emerges for higher values of  $\rho$ ,  $r$  and  $v_0$ ), indicating that the critical exponents depend on the details of the model.

## Acknowledgments

This work was supported by the Brazilian agencies FAPEMAT (Grant No. 685524/2010) and Capes (Grant No. 002/2012).

## References

- [1] J.K. Parrish, L. E-Keshet, *Science* 284 (1999) 99.
- [2] C.W. Reynolds, Flocks, herds and schools, *Comput. Graph.* 2 (1987) 25.
- [3] S. Gueron, S.A. Levin, D.I. Rubenstein, *J. Theoret. Biol.* 182 (1996) 85.
- [4] Ch. Becco, N. Vandewalle, J. Delcourt, P. Poncin, *Physica A* 367 (2006) 487.
- [5] T. Vicsek, A. Czirók, E. Ben-Jacob, I. Cohen, O. Shochet, *Phys. Rev. Lett.* 75 (1995) 1226.
- [6] E.M. Rauch, M.M. Millonas, D.R. Chialvo, *Phys. Lett. A* 207 (1995) 185.
- [7] D.S. Cambui, A. Rosas, *Physica A* 391 (2012) 3908.
- [8] D. Cambui, *Internat. J. Modern Phys. B* 28 (2014) 1450094.
- [9] I. Tarras, N. Moussa, M. Mazroui, Y. Boughaleb, A. Hajjaji, *Modern Phys. Lett. B* 27 (2013) 1350028.
- [10] I. Tarras, M. Mazroui, N. Moussa, Y. Boughaleb, *Modern Phys. Lett. B* 28 (2014) 1450137.
- [11] N. Moussa, I. Tarras, M. Mazroui, Y. Boughaleb, *Internat. J. Modern Phys. C* 22 (2011) 661.
- [12] I. Tarras, M. Mazroui, N. Moussa, Y. Boughaleb, *Int. J. Comput. Appl.* 46 (2012) 21.
- [13] M. Aldana, H. Larralde, B. Vázquez, *Internat. J. Modern Phys. B* 23 (2009) 3661.
- [14] G. Baglietto, E.V. Albano, *Phys. Rev. E* 180 (2009) 050103.
- [15] G. Baglietto, E.V. Albano, *Phys. Rev. E* 78 (2008) 021125.
- [16] M. Nagy, I. Daruka, T. Vicsek, *Physica A* 373 (2007) 445.
- [17] I. Tarras, M. Moussa, M. Mazroui, N. Boughaleb, *Modern Phys. Lett. B* 28 (2014) 1450137.
- [18] K. Binder, D.W. Herrmann, *Monte Carlo Simulation in Statistical Physics: An Introduction*, Springer, Berlin, 1997.
- [19] V. Privman, *Finite-Size Scaling and Numerical Simulation of Statistical Systems*, World Scientific, Singapore, 1990.
- [20] M. Godoy, W. Figueiredo, *Internat. J. Modern Phys. C* 20 (2009) 47.
- [21] M. Henkel, H. Hinrichsen, S. Lübeck, *Non-Equilibrium Phase Transitions: Volume 1: Absorbing Phase Transitions*, Springer, Netherlands, 2008, p. 17.